

# Circuit Schematic of Three-Phase Induction Motor for Use in Cosmic Microwave Background Polarimeter

James Kakos

April 21, 2015

Honors Senior Thesis

Research Adviser: Jeff McMahon

Department of Physics, University of Michigan

## **Abstract**

The theory of inflation is one of the most important ideas in cosmology for explaining problems left unresolved by the Big Bang theory. However, evidence for inflation is currently lacking. One of the sought-after forms of evidence for inflation comes from primordial gravitational waves. These gravitational waves are predicted by inflation to show up as a particular polarization pattern – called a B-mode – in the polarization of the cosmic microwave background. Measuring this B-mode can be done using a rotating half-waveplate. In this paper I lay out the circuit design for a three-phase induction motor that will be used to drive the rotation of a half-waveplate.

# Introduction

Approximately 13.8 billion years ago, the universe unfolded in an event known as the Big Bang. This took the Universe from a high density state to one of rapid expansion. Soon after this event took place, the Universe was composed of a plasma of protons, electrons, and photons. The free electrons scattered photons via Thomson scattering, resulting in an effectively opaque universe. As the Universe continued to expand, it became progressively cooler. Roughly 378,000 years after the Universe began its expansion, it became cool enough to allow for the formation of hydrogen and other light elements. Once this happened, the lack of free electrons meant that photons were able to propagate freely with mean free paths larger than the Hubble length. This event is known as decoupling. The light that was able to propagate freely at the time of decoupling is known as the cosmic microwave background radiation (CMB).

The CMB permeates throughout the Universe with a black body spectrum corresponding to a temperature of 2.725 K. Across the entire sky, the spectrum is uniform to roughly one part in  $10^5$ , and the temperature fluctuates by only  $\pm 200$   $\mu$ K. This isotropy creates a large problem within the standard cosmological model. Photons measured today from the CMB have been traveling for nearly the entire age of the universe to reach us. This means they could not have had enough time to get to regions of the universe on the opposite side from which they came. Within the standard cosmological model, there is no reason that the CMB should be as uniform as it is. This is known as the horizon problem. A leading solution to the horizon problem is inflation.

According to the theory, inflation occurred around  $10^{-36}$  seconds after the Big Bang. During the approximate  $10^{-33}$  to  $10^{-32}$  seconds inflation lasted, the universe expanded exponentially. This exponential expansion can be used to explain not only the horizon problem, but two other problems in cosmology as well: the flatness problem and the magnetic monopole problem. In the flatness problem, we find that the energy density of the Universe would have to be almost exactly equal to the critical energy density during the Planck epoch in order to explain observations of it today. Having an energy density close to the critical energy density makes the Universe flat, but is unstable within the standard cosmological model; any small fluctuations above or below the critical point during the Planck epoch would cause the energy density of the Universe to diverge to either underdense or overdense. The magnetic monopole problem is a prediction of Grand Unified Theories (GUTs). According to GUTs, magnetic monopoles should be dominating the energy density of the Universe, yet not a single magnetic monopole has been observed to date.

Assuming a period of exponential growth in the early universe can solve all three of these problems. First, consider the horizon problem. If a small region of the Universe were in causal contact before inflation, it would be expected that its temperature would be close to uniform. If the Universe grew exponentially for long enough, this uniformity in temperature would be spread across the entire sky, which is what we see in the CMB. Moreover, quantum fluctuations would be expanded to scales that are measurable. These fluctuations have been measured by the Cosmic Background Explorer (COBE) [1], the Wilkinson Microwave Anisotropy Probe (WMAP) [2], and Planck [3]. Another consequence of exponential growth is that the curvature of the Universe becomes stretched out. Similar to the way the Earth appears flat when viewed on scales much smaller than its radius of curvature, the radius of curvature of the Universe becomes so large that the Universe appears flat. Lastly, the rapid growth in volume of the Universe dilutes the number density of magnetic monopoles. This makes them significantly more difficult to detect and it is not surprising that we have yet to find one.

For these reasons, inflation is a very important theory for cosmology, but more evidence for its existence is needed. One of the methods for giving support to inflation is to look for signs of primordial gravitational waves in the CMB. Inflation predicts that a polarization pattern called a B-mode should be found within the polarization of the CMB. This B-mode signal would have originated during inflation, and its detection would not only give support to the theory, but also provide constraints on inflationary models.

To find these patterns in the CMB polarization, we have to look through and remove atmospheric background. The largest source of noise comes from Kolmogorov turbulence. Large eddies form in the air that break down into numerous, smaller eddies. As these eddies dissipate, they create  $1/f$  noise over the weak B-mode signals that need to be detected. Variations in Kolmogorov turbulence show up as fluctuations in temperature, but not polarization. By taking measurements with a rotating half-waveplate, polarized signals will be modulated by some frequency proportional to the rotational frequency of the waveplate. Simultaneously, the background from Kolmogorov turbulence will be reduced to minimal noise when put

into frequency space. This method allows for CMB measurements to be taken despite the large atmospheric background we have to look through. This is the motivation behind the design of this polarimeter.

## Design of the Motor

To simplify the data analysis, we want the waveplate to be spinning at a constant rate while taking measurements. One good way of doing this is to use a superconducting bearing. When a type II superconductor is cooled below a critical temperature, it no longer allows magnetic fields to pass through it. However, in some localized regions within the superconductor, magnetic fields that were present in it before it reached its critical temperature can become trapped. This phenomenon is called flux pinning. If a magnet is held above one of these superconductors before it reaches its critical temperature, it will become locked in place after the superconductor is cooled. The magnet will only be able to move by rotating, which makes it great for use in one of these polarimeters.

Designs for CMB polarimeters using high-temperature superconducting bearings have been used in previous experiments like the E and B Experiment (EBEX) [5] and MAXIPOL [6]. The main differences in these polarimeters comes in the system used to drive the rotation of the waveplate. MAXIPOL used a half-gear to give their rotor a kick and start the rotation. The problem with this is that the rotor cannot be driven and held at a constant rate. The EBEX version improved upon this by using a belt and pulley system attached to the rotor. This allowed them to maintain a rotation frequency but required direct contact with the rotor. The current version of our waveplate spinner was designed to circumvent both of these issues.

The drive for the system is a three-phase induction motor. This allows the rotor to be controlled with no direct contact and also maintain a set rotation frequency. The stator was fitted with three series of solenoids. Each series has a sine wave fed through it to generate magnetic fields that alternate pointing towards and away from the rotor. Magnets were placed on the rotor, going around with their magnetic moments alternating towards and away from the stator. An overview of the rotor and stator system is shown in Figure 1.

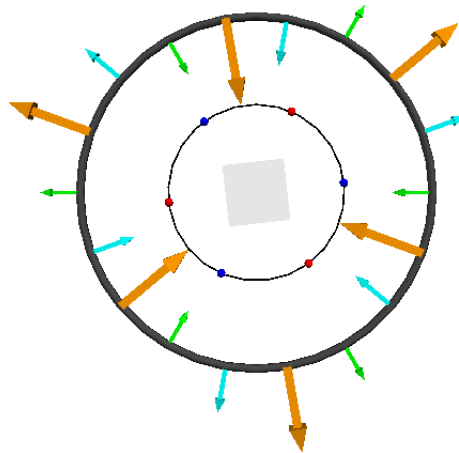


Figure 1: Simulation of the fields of the spinner. The arrows represent the direction and relative strengths of the magnetic fields created by the solenoids. Arrows of the same color are connected with the same input sine wave. The spheres represent magnets attached to the rotor. The opposite colors signify the opposite directions of their magnetic moments along the radial direction. The red spheres are attracted to inward-pointing arrows and blue spheres are attracted to outward-pointing arrows.

In Figure 1, the arrows represent the solenoids attached to the stator and the spheres represent the magnets attached to the rotor. The direction of each arrow indicates the direction of the magnetic field at

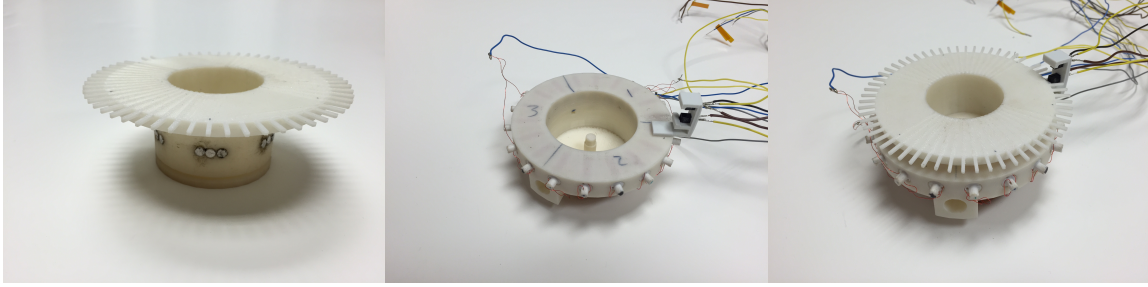


Figure 2: This picture shows the room temperature prototype for the waveplate spinner. A mechanical bearing (not pictured) is placed onto the central peg of the stator (center), and the rotor (left) is fitted onto it. The right picture shows the two pieced together with the spokes of the rotor able to pass through a photogate sensor used for measuring rotor frequencies.

that time, and the relative sizes represent the relative strengths. There are three different colors of arrows that indicate the phase of the sine wave running through that solenoid. For this the rotor to spin smoothly, every other solenoid of a particular phase had its wiring reversed. The spheres fixed to the rotor have two colors to denote the alternating magnetic moments. The red spheres are attracted to arrows that are pointing inwards and the blue spheres are attracted to arrows pointing outwards. This causes a counter-clockwise rotation of the rotor. As time evolves forward, the cyan and orange arrows will decrease in magnitude and the green arrows will increase. They will continue evolve, alternating direction and magnitude sinusoidally. For red spheres, the green arrows across from them will generate an increasing repulsion, pushing the rotor around. The cyan and orange arrows will attract the spheres, pulling the rotor along, as their strengths weaken. It is important for the field strengths to become weaker as the magnets get close to the solenoids in order to avoid slowing and/or stopping the rotation.

The current version of the waveplate spinner is a prototype that operates at room temperature. Pictures of the rotor and stator are shown in Figure 2 [7]. The rotor was fitted with sets of three magnets as opposed to just one in order to broaden the width of the magnetic field and reach adjacent solenoids. Each magnet in a set of three has the same magnetic moment so the functionality is the same as having sets of one magnet. The stator has slots going around its edge inside of which the solenoids are placed. There are 18 solenoids in total – six for each sine wave. As mentioned before, every other solenoid for a given sine wave has its polarization reversed. Every set of six solenoids was split into a series of three wired the one way and three wired the opposite way. These sets of three were wired in parallel to minimize resistance through the solenoids. The rotor was designed with spokes coming off the upper edge for measuring rotational frequencies. A photogate sensor was attached to the stator which could read out its signal to an oscilloscope for analyzing.

## The Circuitry

To get the waveplate spinner to rotate properly, three out-of-phase sine waves with equal frequencies were run through the three sets of solenoids. The necessary waves were  $\sin(\vartheta)$ ,  $\sin(\vartheta + 60)$ , and  $\sin(\vartheta + 120)$  (Note that  $\sin(\vartheta + 60)$  is equivalent to  $-\sin(\vartheta + 240)$ ). In the remainder of this paper, this specific wave will be referred to as  $-\sin(\vartheta + 240)$ . To create these waves, the following trigonometric identity was used

$$\sin(\alpha + \beta) = \sin(\alpha) \cos(\beta) + \cos(\alpha) \sin(\beta) \quad (1)$$

Using  $\beta$  as the phase angle, it is clear that each of the phased sine waves is a sum of non-phased sine and cosine waves with the appropriate amplitudes. In order to get the three final sine waves, first a sine and a cosine wave had to be generated. These waves were made using the schematic shown in Figure 4 [4]. This circuit takes in a DC voltage,  $E_C$ , from 0.1 to 10 V and generates a sine and a cosine wave at two pins. Typically, for a stable spin, the input voltage is kept between 0.5 V and 2 V. In the current state of this circuit, capacitors C1 and C3 have been swapped out for capacitors with capacitances of 0.22  $\mu\text{F}$ . These two capacitors have a direct effect on the frequency of the output waves. A test was done using five different



capacitors and the results are shown in Figure 3. It was found that the signal frequency scales inversely proportionally to changes in the capacitances of C1 and C3.

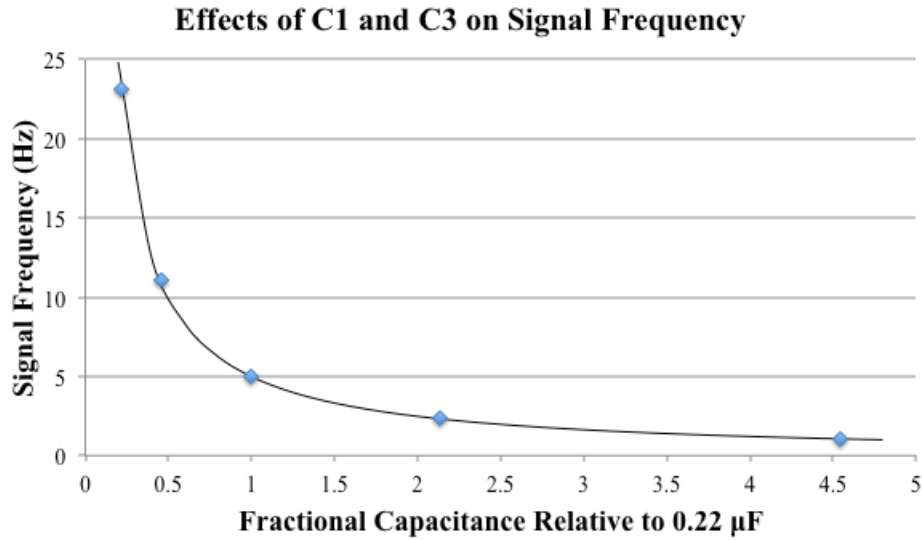


Figure 3: Signal frequency behavior with changes in capacitors C1 and C3. The x-axis shows fractional changes in capacitance relative to the 0.22 μF capacitors currently in the circuit. As an example, going out to 2 on the x-axis would correspond to doubling the capacitance of each capacitor and consequently halving the signal frequency.

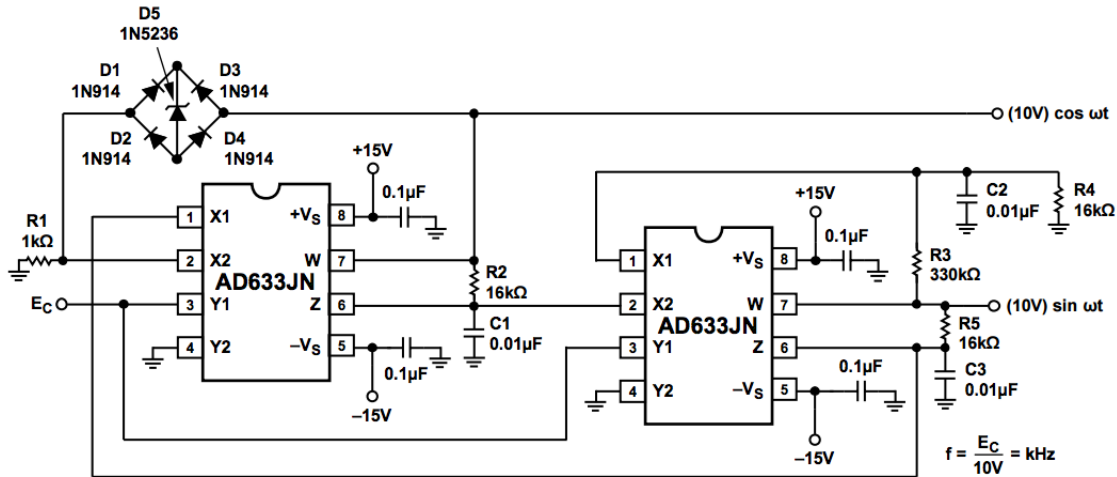


Figure 4: Circuit layout that generates a sine and cosine wave. Capacitors C1 and C3 can adjust the frequency of the outgoing waves. Changes in these capacitances will inversely change the frequency of the outgoing signals.

The first part of the sine and cosine wave adjustments is shown in Figure 5. This chip, as with the remaining chips in the circuit, is a set of operational amplifiers (op amps). The specific chip used in this circuit is written at the top of edge of the drawing, but any op amp will work. Pin 2 takes in the sine wave which goes through the inverting terminal of the op amp. The resistors here are used for scaling down the amplitude of the wave. After running through the op amp, the sine wave will exit at pin 1 and have its sign flipped. This is needed for the next stage of the circuit. On the other side of the chip, the cosine wave is also

passed through the inverting terminal on the second op amp. Its amplitude is scaled down to match that of the sine wave. It exits at pin 7 with a sign flip, like the sine wave.

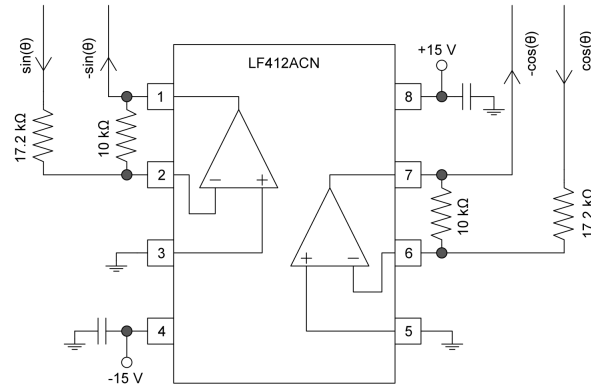


Figure 5: This chip takes in the sine and cosine waves and flips them to be negative. These flips are in preparation of the signal addition that takes place in the chip that follows.

The next stage of the circuit is shown in Figure 7. The left op amp of this chip will be making the sine wave that has the 240 degree phase shift. Equation 1 says that this wave can be made by the following

$$\sin(\vartheta + 240) = -\frac{1}{2} \sin(\vartheta) - \frac{\sqrt{3}}{2} \cos(\vartheta) \quad (2)$$

The first stage of the circuit produced negative sine and cosine waves, so only amplitude scaling needed to be taken care of here. The waves will be added using an inverting summing amplifier. A general schematic for this type of amplifier is shown in Figure 6. The equation for  $V_3$  in this setup is given by

$$V_3 = -R_3 \left( \frac{V_1}{R_1} + \frac{V_2}{R_2} \right) \quad (3)$$

For simplicity,  $R_3$  was set to  $1 \text{ k}\Omega$ . Scaling the sine was down by a factor of one-half becomes easy and required only that  $R_1$  is set equal to  $2 \text{ k}\Omega$ . Scaling the cosine wave is not as trivial because  $\sqrt{3}$  is irrational. A  $2 \text{ k}\Omega$  trimmer potentiometer (trimpot) was used as a variable resistor to get around this. According to the above equations,  $R_2$  should be set to  $2/\sqrt{3} \text{ k}\Omega$ , which is approximately  $1.15 \text{ k}\Omega$ . When adjusting the trimpot, I read out the sine and phase-shifted sine waves to an oscilloscope. The trimpot was adjusted until the amplitudes of both waves matched. I found that setting the trimpot to  $1.3 \text{ k}\Omega$  gave the best result. After these scaled sine and cosine waves run through the inverting summing amplifier, pin 1 will send out a  $-\sin(\vartheta + 240)$  wave. The second op amp, on the right side of the chip, is setup as a voltage follower for the negative sine wave. An op amp setup this way draws very little current and acts as a voltage source for this wave. This was added in because this negative sine wave will be needed again in coming stages of the circuit.

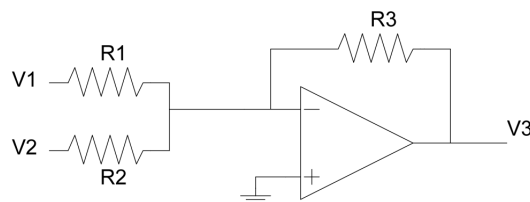


Figure 6: This figure shows a general inverting summing amplifier.

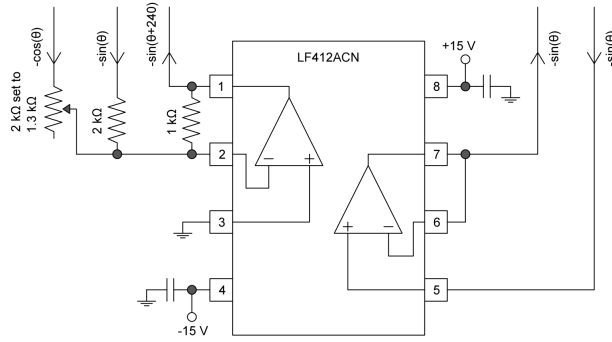


Figure 7: This chip scales the sine and cosine waves and then adds them to generate a  $-\sin(\vartheta+240)$ . It also makes a voltage follower for the  $-\sin(\vartheta)$  which will go on to make the  $\sin(\vartheta+120)$  wave.

The next stage of the circuit generates the third and final phased sine wave needed to drive the motor. The schematic for this chip is shown in Figure 8. As on the previous chip, the left op amp is arranged as an inverting summing amplifier. This case is more convenient than the previous one, though, in that adding  $[-\sin(\vartheta)] + [-\sin(\vartheta + 240)]$  directly gives  $\sin(\vartheta + 120)$ . The resistors used here were  $2.2\text{ k}\Omega$  resistors, but these can be swapped out for other resistors so long as they have equal resistances. The third resistor was replaced with a trimpot in order to allow for some fine tuning of the amplitude of the  $\sin(\vartheta + 120)$  output. Since no scaling is necessary when adding the  $-\sin(\vartheta)$  and  $-\sin(\vartheta + 240)$  waves together, the trimpot should theoretically be set to  $2.2\text{ k}\Omega$  to match the other two resistors. In practice, however, I found that the best result came from setting the trimpot to  $2.3\text{ k}\Omega$ . The second op amp in this chip is unused.

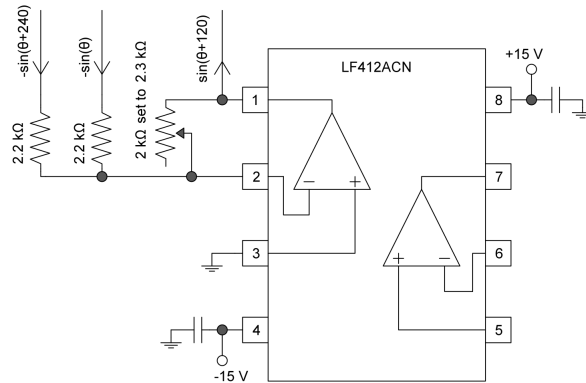


Figure 8: This chip adds the  $-\sin(\vartheta)$  and  $-\sin(\vartheta+240)$  waves to get out a  $\sin(\vartheta+120)$  wave.

The final stage of the circuit amplifies the signals before sending them into the solenoids. Each signal is sent through a power op amp like the one shown in Figure 9. These op amps are able to deal with higher currents than other chips in the circuit so they are added in last. The signals happen to be connected to the inverting terminals of the op amps, but they could just as well be connected to the non-inverting terminals. As long as all three waves are sent through the same terminal on each op amp, the resulting waves will be effectively the same. At the output, there are three resistors wired in parallel. This wiring is done to decrease the current through each one and avoid frying the part. This set of three resistors can be replaced by a single power resistor capable of handling the higher current at that point. The signal coming out of these resistors is the final signal that gets wired directly to the solenoids in the stator.

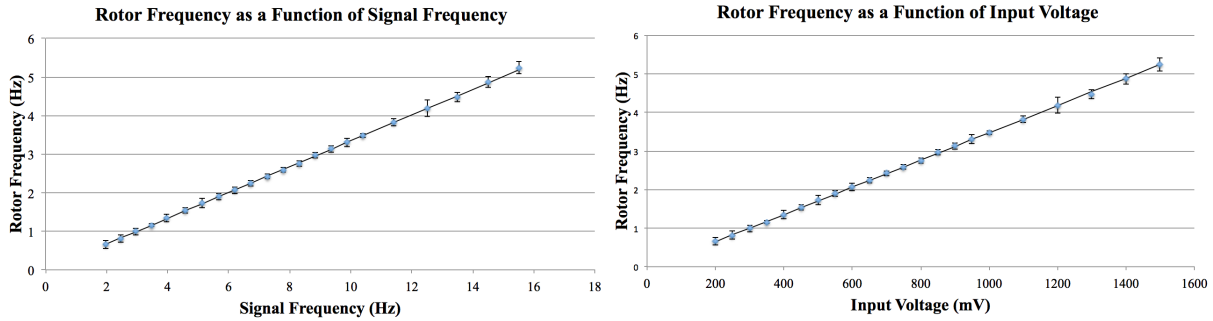


Figure 10: These graphs show the behavior of the rotor frequency with respect to the signal frequencies and input DC voltage.

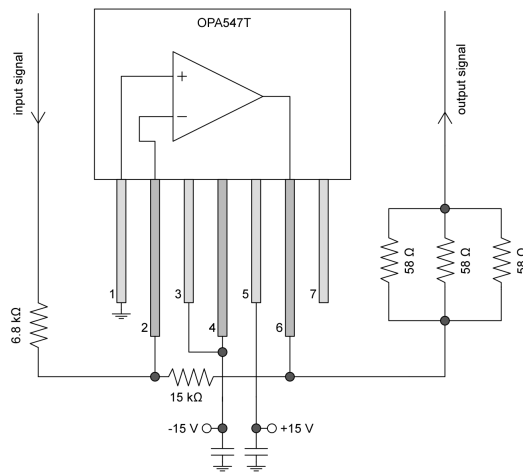


Figure 9: This chip is a power amplifier used to boost the wave signals before going into the solenoids.

## Performance

A few tests were run to take a look at how the signals, input voltage, power supply voltage, and rotor frequency are related. The first two tests are shown in Figure 10. These tests show how the frequency of the rotor changes with the frequencies of the sine waves, as well as with the voltage of the DC input. These tests were run with a power supply voltage of 7V. In both cases, there is a strong linear relationship. By construction of the three-phase motor, it was expected that the rotor frequency should be one-third of the signal frequency. In this test, the data was fit to a straight line and the slope was determined to be  $0.335 \pm 0.005$ .

The next test looked at the change in amplitude of the sine waves as the power supply voltage changed. The relationship also appears linear and is shown in Figure 11. One interesting feature of this test was that it showed a region of power supply voltages that distort the signals. The signals maintain a sinusoidal shape for power supply voltages ranging from 3V to 7V. Beyond 7V, the waves begin to get cut off near the peaks and flatten out. Once the power supply voltage reaches 15V, the signals once again follow a sinusoidal shape. Three images of the signals are shown in Figure 12 for 7V, 10V, and 15V. The cause of the cut off in the signals is unclear. Additionally, setting the power supply to 15V seems to be too high for parts of the circuit to handle, despite many of the chips operating at this voltage. Since the sine waves are still well-behaved for

7V and lower, the circuit is typically powered at 7V in order to maximize the amplitudes, minimize heating, and maintain well-formed signals.

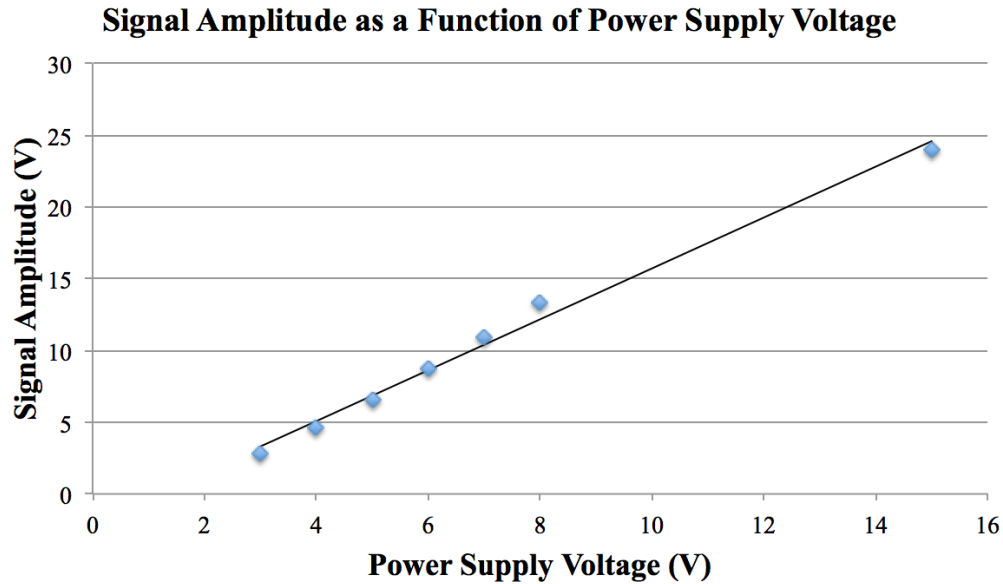


Figure 11: This graph shows the relationship between the signal amplitude and the power supply voltage. Data was taken over ranges where the sine waves can still maintain their shapes. One point was taken outside of this range, at 8V, and is the point that deviates the most from linear fit.

The main obstacle with the current state of the wave spinner is getting the rotor into a stable rotation from a standstill. So far, two different methods have been successful in achieving this but neither is exceptionally reliable. The first method is to start the input voltage at 0V and increase it by roughly 10 mV per second. This method is only successful roughly 10% of the time it is attempted. When the rotor is at a standstill and trying to get into a stable rotation, it is susceptible to sudden kicks when the magnetic fields from the solenoids hit a maximum near the rotor magnets. It seems the best chance of locking the rotor into a stable rotation is when one of these kicks puts it at a frequency comparable to a third of the signal frequency. The second method is to essentially simulate one of these kicks by hand. Setting the input voltage somewhere between 500 mV and 1000 mV and then spinning the rotor by hand can usually be successful in achieving a stable rotation roughly 20% of the time.

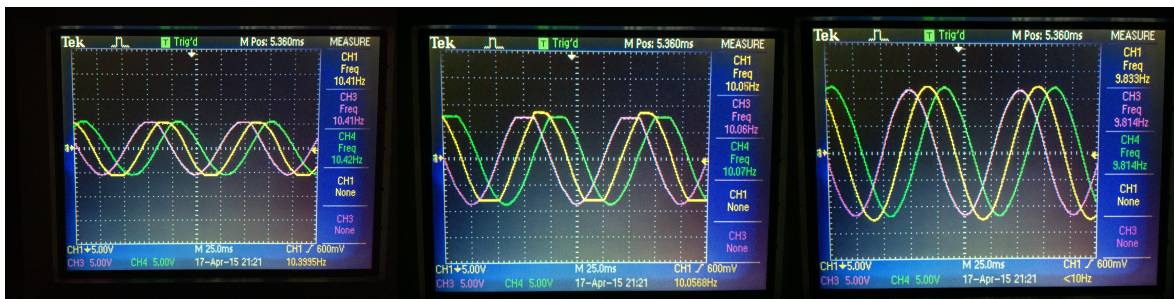


Figure 12: These three images show the output waves for different powering voltages of the circuit. From left to right, the voltages are 7V, 10V, and 15V.

Once the rotor makes it to a stable rotation, however, it performs very well. Through all testing of the wave spinner, given a constant power supply voltage and input voltage, it has never fallen out of its rotation. One test was done to see how long it could maintain a stable rotation. It lasted approximately 20 hours.

before being shut off. It is not limited to constant input voltages, though. The data taken for the rotor frequency as a function of input voltage was all collected while maintaining a single, stable rotation. The rotor was put into rotation around 500 mV, brought up to 1500 mV, and then brought back down to 200mV to collect data. So far, the lowest frequency the wave spinner has been able to maintain is about 0.66 Hz, which occurred at a 200 mV input. The issue at lower frequencies comes down to the quality of the sine waves. Once the input voltage drops around 350 mV, the sine waves begin to drift and lose their symmetry about the line  $y = 0$ . The wave spinner is resilient enough to withstand these deviations down to 200 mV, but no lower as of yet.

## Future Adjustments

So far, the vast majority of testing for this circuit has been done on the room temperature model of the waveplate spinner shown in Figure 2. Recently, a new version of the spinner has been made but has undergone very limited testing. A picture of this version is shown in Figure 13 [7]. A successful, stable rotation has not yet been achieved in this model. The main issue seems to be with the bearing generating much more friction than expected. A replacement bearing is needed before any final conclusions can be made regarding this model's ability maintain a stable rotation. In addition to room temperature operation, this model is also designed for cryogenic testing with a superconducting bearing. If the main issue with this model is due to the mechanical bearing, cryogenic testing with the near-frictionless superconducting bearing bodes well for successful operation in the future.

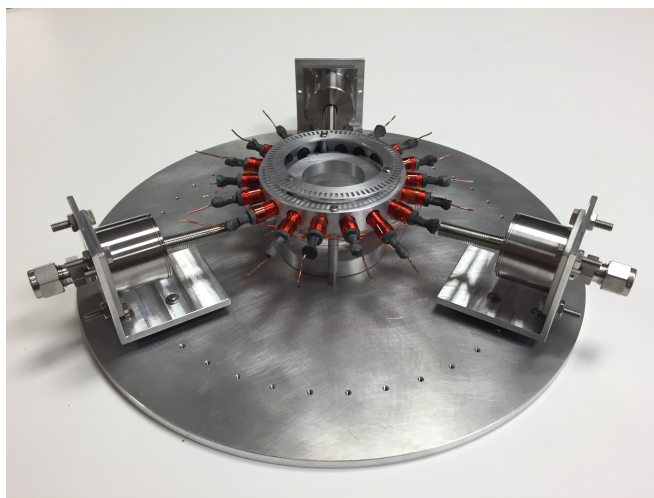


Figure 13: This picture shows the first version of the waveplate spinner that will be tested cryogenically. The rotor is held suspended above the base plate where the superconductor will be placed. Once the system is cooled to cryogenic temperatures, the rotor will become locked in place as a result of flux pinning created the by the superconductor and a magnet attached to the underside of the rotor.

The next step to take with the circuit is to be able to operate it from a computer rather than by hand. The current plan is to be able to remotely control the input DC signal. The process of increasing the voltage at a rate of roughly 10 mV per second is the best bet at this point since it has already been shown to work in the past. Attaching a photogate sensor to monitor the rotational frequency of the rotor would allow us to know if a stable rotation has been achieved or if the process needs to be restarted. Since the most successful method of getting a stable rotation has been spinning the rotor by hand, another promising direction to move in would be simulating this initial kick. So far, no consistent means of accomplishing this have been worked out.

## References

- [1] Cosmic Background Explorer, <http://lambda.gsfc.nasa.gov/product/cobe/>
- [2] WMAP Produces New Results, <http://map.gsfc.nasa.gov/news/>
- [3] Planck Publications, <http://www.cosmos.esa.int/web/planck/publications>
- [4] <http://www.analog.com/media/en/technical-documentation/data-sheets/AD633.pdf>
- [5] Proc. of SPIE Vol. 8150 815004-1
- [6] IEEE Transactions on Applied Superconductivity, Vol. 13, No. 2, June 2003
- [7] Chris Richard, Prototype Cryogenic Induction Motor for use in a Cosmic Microwave Background Polarimeter, B.S., University of Michigan (2015)